

# **Tailoring wettability through the surface modification of electro-spun polymers by plasma and sol-gel treatments**

Damon Gilmour, Ryan Glendinning, Bruce Kaye, Paul Saville

**Defence Research and Development Canada**

Scientific Report

DRDC-RDDC-2014-R102

November 2014

- © Her Majesty the Queen in Right of Canada, as represented by the Minister of National Defence, 2014
- © Sa Majesté la Reine (en droit du Canada), telle que représentée par le ministre de la Défense nationale, 2014

## Abstract

---

The interaction of liquids with a material's surface is of fundamental importance to many processes including adhesion, chemical reactions, hydrodynamic transport, and surface cleanability. Surface properties can range from being hydrophilic, or oleophilic, where the liquid wets the surface and spreads, to superhydrophobic, or oleophobic, where the liquid beads on the surface and is easily displaced. The requirements for a surface to be superhydrophobic or oleophobic are low surface energies and minimal contact between the liquid and surface, which is often created by micron and nanometer scale roughness. In this work, solutions of polyurethane and polyvinylidene difluoride-co-hexafluoropropylene were electrospun to create mats of micron-sized fibres. Secondary roughness was added to the polymer fibres through the use of microphase separation, incorporation of nanoparticles, sol-gel reactions and by producing beads-on-a-string morphologies. Low surface energy was added by using fluorinated polymers, or through sol-gel reactions with low surface energy alkyl siloxanes, and plasma polymerization was attempted. Water contact angles of spun fibre mats were typically in the range of 110-130° which is hydrophobic, but the water drops were often pinned to the surface by fibres penetrating the drops. Sol-gel coatings resulted in water contact angles > 150° and very small tilt angles. Argon plasma treatment of the fibres resulted in water drops completely wetting the surface with very small contact angles. Better mass flow control of the monomer is required for plasma polymerization. Fibres were characterized by contact angle measurement with a digital microscope; scanning electron microscopy; FTIR and EDX spectroscopy.

## Significance to defence and security

---

The ability of a liquid to wet and adhere to the surface of a material is fundamental to many defence applications, including: adhesives; decontamination of equipment exposed to chemical agents; general cleanability of materials; personnel comfort – rainwear and tents; anti-icing coatings for aircraft and ships; hydrodynamic flow; and anti-biofouling.

## Résumé

---

L'interaction de liquides avec la surface des matériaux est d'une importance fondamentale pour de nombreux processus, dont l'adhésion, les réactions chimiques, le transport hydrodynamique et la nettoyabilité des surfaces. Les propriétés des surfaces peuvent se situer dans une gamme allant d'un caractère hydrophile ou oléophile, quand le liquide mouille la surface et s'étale, à un caractère superhydrophobe, ou oléophobe, quand le liquide perle à la surface et est facilement déplacé. Les conditions pour qu'une surface soit superhydrophobe ou oléophobe sont une faible tension superficielle et un contact minimal entre le liquide et la surface, qui est souvent créé par une rugosité à l'échelle micrométrique ou nanométrique. Pour le présent travail, nous avons électrofilé des solutions de polyuréthane et de poly(difluorure de vinylidène-co-hexafluoropropylène) afin de créer des mats de fibres micrométriques. Une rugosité secondaire a été ajoutée aux fibres de polymère grâce à l'utilisation d'une séparation de microphase, à l'incorporation de nanoparticules, à des réactions sol-gel et par la production de formes semblables à des perles enfilées. On a introduit une faible tension superficielle en utilisant des polymères fluorés ou grâce à des réactions sol-gel avec des alkylsiloxanes de faible tension superficielle, et tenté une polymérisation sous plasma. Les angles de contact avec l'eau des mats de fibres filées étaient typiquement dans la gamme 110-130°, ce qui est hydrophobe, mais les gouttelettes d'eau étaient souvent liées à la surface par des fibres les traversant. Les revêtements sol-gel ont produit des angles de contact avec l'eau > 150° et de très petits angles de déversement. Le traitement des fibres au plasma d'argon a formé des gouttelettes d'eau mouillant complètement la surface avec de très petits angles de contact. Un meilleur contrôle du débit massique du monomère est requis pour la polymérisation sous plasma. Les fibres ont été caractérisées grâce à des mesures de l'angle de contact par microscopie numérique, par microscopie électronique à balayage, par spectroscopie IRTF et EDX.

## Importance pour la défense et la sécurité

---

La capacité d'un liquide à mouiller la surface d'un matériau et à y adhérer est fondamentale pour de nombreuses applications de défense, dont les adhésifs, la décontamination de l'équipement exposé à des agents chimiques, la nettoyabilité des matériaux en général, le confort personnel – vêtements de pluie et tentes, les revêtements antigivrage pour les aéronefs et les navires, l'écoulement hydrodynamique et l'anti-encrassement biologique.

# Table of contents

---

Abstract .....	i
Significance to defence and security .....	i
Résumé .....	ii
Importance pour la défense et la sécurité .....	ii
Table of contents .....	iii
List of figures .....	iv
List of tables .....	vi
Acknowledgements .....	vii
1 Introduction .....	1
1.1 Fabrication by electrospinning .....	4
1.2 Plasma treatment .....	4
1.3 Sol-gel coatings .....	6
2 Materials and methods .....	7
2.1 Electrospinning .....	7
2.2 Plasma treatment .....	7
2.3 Sol-gel coatings .....	8
2.4 SEM imaging .....	9
2.5 ATR FTIR spectroscopy .....	9
2.6 Contact angles .....	9
3 Results and discussion .....	10
3.1 Fabrication by electrospinning .....	10
3.2 Roughness and derivatization .....	13
3.2.1 Microphase separation of electrospun polymer blends .....	13
3.2.2 Electrospinning with nanoparticles .....	13
3.2.3 Effect of TEOS addition to electrospinning solutions .....	14
3.2.4 FTIR spectroscopy of electrospun fibres .....	15
3.3 Sol-gel coatings .....	16
3.3.1 FTIR spectroscopy of sol-gel coated polymer fibres .....	18
3.3.2 Energy dispersive X-ray analysis of polymer and sol-gel coatings .....	19
3.3.3 Contact angle measurements .....	19
3.4 Plasma treatment .....	21
4 Conclusions and future work .....	24
References .....	25

## List of figures

---

Figure 1	Surface tension diagram of a free water droplet on a hydrophobic surface. ....	1
Figure 2	Wenzel and Cassie-Baxter model surfaces. ....	2
Figure 3	Self-cleaning effect of a Cassie-Baxter water drop interaction.....	3
Figure 4	Repeating unit of (top) polyurethane and (bottom) polyvinylidene fluoride-co-hexafluoropropylene. ....	4
Figure 5	Plasma-enhanced chemical vapour deposition PECVD mechanism. ....	6
Figure 6	Base catalyzed hydrolysis of general silane, $\text{Si(OR)}_4$ . ....	6
Figure 7	Sol-Gel precursors, (left) FAS, (right) Tetraethyl orthosilicate. ....	7
Figure 8	Plasma reactor schematic for PECVD, for plasma treatment no monomer reservoir is used. ....	9
Figure 9	Electrospun mat from a solution containing 12% PU and 2% TEOS w/v in 60/40 THF/DMF, 35 cm working distance, 30 $\mu\text{L}/\text{min}$ flow rate, 20 gauge needle, 16 kV ....	11
Figure 10	Electrospun mat from a solution containing 15% PVDF-co-HFP and 2% TEOS w/v in 75/25 DMF/Acetone, 35 cm working distance, 30 $\mu\text{L}/\text{min}$ flow rate, 20 gauge needle, 20 kV ....	12
Figure 11	Effect of flow rate for electrospun 9.5% polyurethane in 60/40 THF/DMF. (left) 25 $\mu\text{L}/\text{min}$ , (right) 50 $\mu\text{L}/\text{min}$ , at a working distance of 35 cm, 20 gauge needle, 13 kV.....	13
Figure 12	SEM image of electrospun 10% polyurethane with 4% PVDF-co-HFP. The fibres appear to be rough with white nodules. ....	14
Figure 13	SEM image of electrospun polyurethane with 1% $\text{TiO}_2$ . $\text{TiO}_2$ particles are visible as white particulate clusters on the fibre surface. ....	15
Figure 14	Left, 9.5% polyurethane, and right 10% polyurethane + 4% TEOS electrospun fibres from 60/40 THF/DMF, 35 cm working distance, 20 gauge needle, 15-20 kV +, 10 kV - collector, 25-30 $\mu\text{L}/\text{min}$ flow rate.....	15
Figure 15	FTIR Spectra.....	16
Figure 16	FTIR Spectra.....	17
Figure 17	Electrospun polyurethane + TEOS, before and after coating in 1 ..... 18	18
Figure 18	Electrospun PVDF-co-HFP + TEOS mat coated in 1 ..... 18	18
Figure 19	ATR-FT-IR Spectra ..... 19	19
Figure 20	ATR-FT-IR Spectra of 15% PVDF-co-HFP + 2% TEOS, red line, and sol-gel coated 15% PVDF-co-HFP + 2% TEOS, blue line..... 20	20
Figure 21	A 5 $\mu\text{L}$ water drop on electrospun polyurethane + TEOS before coating, left, and after coating with the sol-gel, right. The contact angles are $131^\circ$ and $162^\circ$ respectively. .... 21	21

Figure 22	A 5 $\mu$ L water drop on electrospun PVDF-co-HFP + TEOS before coating, left, and after coating with the sol-gel, right. The contact angles are 134° and 170° respectively. ....	22
Figure 23	A modified PECVD set-up. ....	24

## List of tables

---

Table 1	Composition of polyurethane and PVDF-co-HFP, electrospun with TEOS, before and after coating with FAS sol-gel as measured by EDX.....	20
Table 2	Contact angle measurements for polymers before and after sol-gel coating. ....	22



## Acknowledgements

---

The Authors would like to acknowledge the support of Michael Kopac and Brad Noren in material analysis and characterization.

This page intentionally left blank.

# 1 Introduction

---

Across the scientific landscape much of human innovation has resulted from biomimicry, the examination of nature for the purpose of modelling and solving technical challenges. A fascinating example is the lotus leaf, thought of for thousands of years as a symbol of purity, due to its clean appearance upon emerging from muddy water, within which it grows. In the latter half of the 21<sup>st</sup> century, the mechanism behind this feature was described as self-cleaning and dubbed the ‘lotus effect’ by Barthlott.<sup>1</sup> It was found to arise from a waxy, three dimensional surface structure on the leaf’s surface, giving it a property referred to as superhydrophobicity. Water on superhydrophobic materials bead up, with drops exhibiting static contact angles exceeding 150°, and they roll off at a very low tilt angles.<sup>2</sup>

A drop of liquid will adopt an equilibrium shape as surface tensions are balanced and free energy minimized. Young’s equation is the thermodynamic expression relating the surface tensions: solid-vapour, solid-liquid and liquid-vapour,  $\gamma_{SV}$ ,  $\gamma_{SL}$  and  $\gamma_{LV}$ , respectively:

$$\gamma_{SV} = \gamma_{SL} + \gamma_{LV} \cos \theta \quad (1)$$

Where the contact angle,  $\theta$ , is the angle formed between the solid-liquid interface and the tangent line of the liquid-vapour interface at the three phase boundary, Figure 1.

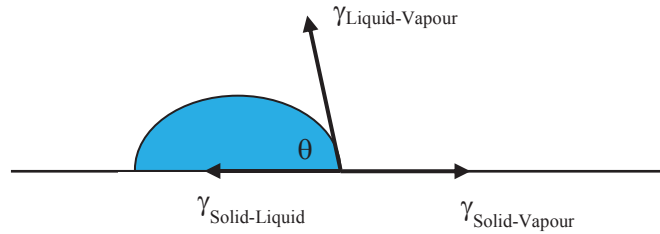


**Figure 1:** Surface tension diagram of a free water droplet on a hydrophobic surface.

If the solid-vapour surface tension is greater than the solid-liquid surface tension,  $\gamma_{SV} > \gamma_{SL}$ , then the contact angle is less than 90 degrees. If the solid-vapour surface tension is less than the solid-liquid surface tension,  $\gamma_{SV} < \gamma_{SL}$ , then the contact angle is greater than 90 degrees. Finally, if the solid-vapour and solid-liquid surface tensions are equal in magnitude, the liquid adopts a spherical shape and the contact angle is 180 degrees. This is the same as if the droplet is suspended in air.

The magnitude of the surface tension depends on the chemical nature of the materials that are in contact. Polar species tend to have high surface tension (or surface energies), examples being water, glasses, and metals. Non-polar species have low surface tension, for example PTFE and hydrocarbons. Polar species may interact through strong hydrogen bonding, while non-polar species interact through weaker van der Waals forces, which are not strong enough to cause the

liquid to wet the surface and spread. Low surface energy materials are more likely to result in the liquid forming a bead.

For superhydrophobic materials such as the lotus leaf, it has been noted that in addition to the presence of low surface energy waxy materials, the surfaces are rough, on a micro- and nano-scale.<sup>3</sup> Two models have been developed for describing the interaction of liquids with rough surfaces, where the liquid either wets the surface forming a conformal interface, or the liquid rests on top of the surface roughness, Figure 2.<sup>4</sup>

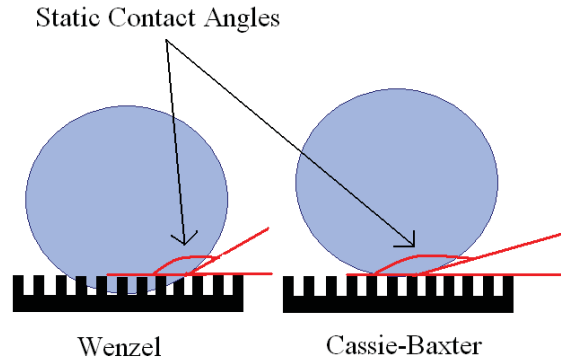


**Figure 2:** Wenzel and Cassie-Baxter model surfaces.

When the liquid wets the rough surface, forming a conformal interface it is termed the Wenzel state. The contact angle observed,  $\theta_w$ , for the drop on the rough surface is related to the contact angle on a smooth surface,  $\theta$ , by:

$$\cos\theta_w = r\cos\theta \quad (2)$$

Where  $\theta_w$  is the Wenzel state contact angle,  $r$  is the true surface area divided by the projected area, and  $r \geq 1$ . This relationship shows that the observed contact angle of water on a hydrophilic surface ( $\theta < \pi/2$ ) will be smaller, than on a smooth surface. Conversely the observed contact angle will be larger for water on a hydrophobic surface ( $\theta > \pi/2$ ).

The second state is the Cassie-Baxter model, where the liquid rests on top of the surface roughness, trapping air underneath. The contact angle is then expressed in terms of the fraction of the surface in contact with water,  $f$ , and is represented by:

$$\cos\theta_{CB} = f\cos\theta_{water} + (1 - f)\cos\theta_{air} \quad (3)$$

Where  $\theta_{CB}$  is the Cassie-Baxter state contact angle and  $\theta_{air}$  is the air contact angle. Since  $\theta_{air}$  is  $180^\circ$ , Equation 3 can be simplified to:

$$\cos\theta_{CB} = f(1 + \cos\theta_{water}) - 1 \quad (4)$$

This relationship indicates that it is possible for the surface to have a high contact angle even if it is hydrophilic, though this specific condition is metastable and can transition to the Wenzel state.

It is possible to achieve stable contact angles greater than  $150^\circ$  on superhydrophobic material through the combination of low surface energy material and surface roughness, as observed for the lotus leaf.

A liquid that is in the Wenzel state (conformal with the solid) may be pinned to the surface even if a large contact angle exists. This is a consequence of the work of adhesion, large contact area, and the energy required to form a liquid-free surface. In contrast, liquid drops on a Cassie-Baxter surface have a small contact area with the surface, and if the surface is non-polar, then the work of adhesion is small and the drops may roll on the surface in response to small forces, such as gravity.

A drop of liquid on a Cassie-Baxter surface can give rise to a special property referred to as self-cleaning, also known as the lotus effect. Self-cleaning arises when the drop on the Cassie-Baxter surface rolls off. “Dirt” on the surface can adhere to the drop and if the solid surface is inclined enough to cause the drop to roll, the dirt will be carried away; thus the name self-cleaning. In order for this to work, the adhesion of the dirt to the liquid has to be greater than the adhesion of the dirt to the surface.

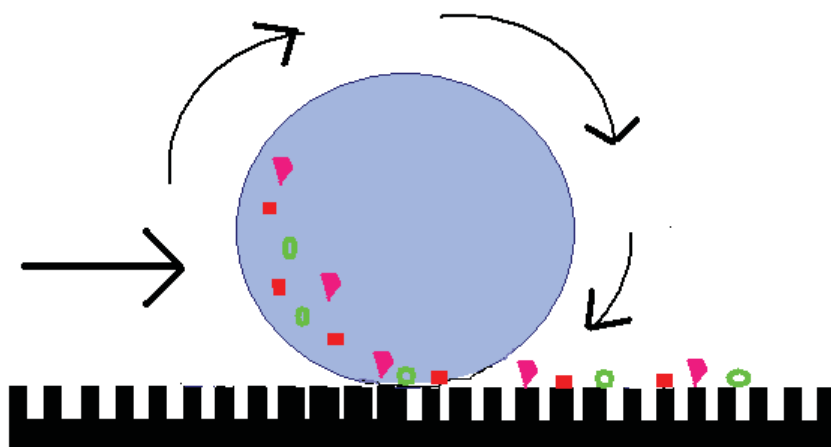


**Figure 3:** Self-cleaning effect of a Cassie-Baxter water drop interaction.

Realization of superhydrophobic surfaces could benefit a number of applications: anti-biofouling; corrosion resistant paints for hulls; coatings that prevent ice buildup; water, stain and oil resistant textiles; and self-cleaning surfaces for windows and exteriors.<sup>5</sup>

In order to make a self-cleaning super hydrophobic/oleophobic surface, the requirements include low surface energy, and surface roughness. Polymeric materials offer a wide range of chemical and mechanical properties and can be fabricated in different forms. Electrospinning is one technique for producing a mat of fibres with micron sized diameters. Such a mat should have the requisite roughness for a superhydrophobic/oleophobic surface. The surface energy of the fibre mat can be tuned based on the chemical composition of the polymer(s) used. Alternatively, the surface of electrospun polymer fibre mats, with good mechanical properties and high surface energy, can be derivatized with low surface energy coatings. Plasma polymerization is one method for applying a thin conformal low surface energy coating onto the fibres, while chemical derivatization is another.<sup>6,7</sup> Additional surface roughness can be added by electrospinning the fibres with nanoparticles in the solution or melt, or by using a sol-gel process to deposit low

energy colloidal particles onto the surface. These strategies are elaborated on in the next sections and have been used to make rough low surface energy materials for the purpose of studying superhydrophobic/oleophobic materials.

## 1.1 Fabrication by electrospinning

Given that a superhydrophobic material must possess micro-roughness, the electrospinning of polymer mats of nanometer to micron-sized fibres is a means of fabricating a rough surface.<sup>8</sup> Electrospinning occurs when a high voltage is applied to a polymer solution in a syringe needle. The charge from the high voltage accumulates on the surface of the polymer solution at the needle tip, causing it to deform into a conical shape referred to as a Taylor cone. When the repulsive forces on the surface exceed the surface tension, a fine jet of polymer solution is ejected from the liquid surface. This jet of liquid becomes unstable, and whips around, leading to extension (thinning) and solvent evaporation. Fibres collect on a grounded or oppositely charged plate. Using this technique, mats of nanometer to micron-sized polymer fibres can be produced, yielding the roughness scale required for superhydrophobicity.

To analyze the effect of surface energy on water repellency of electrospun materials, two polymers with different surface energies were used: polyurethane containing urethane and phenyl groups has high and low surface energy regions due to its composition and falls between the hydrophilic and hydrophobic extremes; and the second polymer, polyvinylidene fluoride-co-hexafluoropropylene (PVDF-co-HFP), has significant fluorination and as a consequence, low surface energy, Figure 4. In addition, fibres were spun from solutions of these polymers with tetraethyl orthosilicate (TEOS), with the intent that via sol-gel chemistry the TEOS would form functionalization sites on the polymer fibre and increased fibre roughness. These polymer solutions were easily electrospun into nano-/microfibres, with high surface area and roughness.

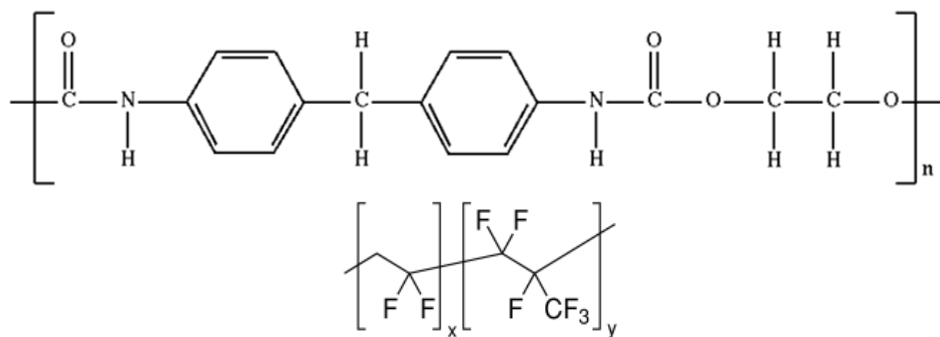


**Figure 4:** Repeating unit of (top) polyurethane and (bottom) polyvinylidene fluoride-co-hexafluoropropylene.

## 1.2 Plasma treatment

Plasmas are formed via application of an electric potential across a gas. The electrical field causes charge separation to occur; pulling electrons toward the positive anode and the nuclei toward the negative cathode. At a sufficiently high potential gradient, electrons will be separated from the

atom (dielectric breakdown) and the insulating dielectric gas will become a conductor.<sup>9</sup> As the ionization proceeds, increasing numbers of collisions between charged and neutral species prompts further ionization. The medium will reach thermal equilibrium once the electrons and heavier atoms and ions are at the same temperature, due to the vast number of electrons elastically colliding with heavier particles. This medium of charged particles is a plasma. The high energy electrons in the plasma can cause radical formation in a material it contacts and molecular fragments can recombine forming polymeric films.

Plasmas can be generated under a range of conditions, including direct or alternating current, at radio- or microwave frequencies, and pressures ranging < 1 Torr to atmospheric (760 Torr). Plasmas are described based on the degree of ionization: for hot plasmas the gas is nearly completely ionised, while for cold plasmas the gas is only partially ionized.<sup>6</sup> One advantage of a cold plasma is that low melting materials such as polymers can be exposed to the plasma without significant damage.

Research has been conducted on the nature of plasma interactions with surfaces. Surface modifications can include chemical etching, deposition of sputtered radical ions or charged fragments, and bond dissociation by UV radiation.<sup>10</sup> It is also possible to generate oxygen containing functional groups such as hydroxyls (-OH) and carbonyls (C=O) at the surface, as a result of free radical reactions at the surface, and subsequent reaction with ions or upon exposure to atmospheric oxygen. Sites of the polymer chain containing radicals can also combine and cross-link, while smaller scission products can be sputtered and evaporated off the surface. The generation of polar groups and radicals on the surface increases its surface energy, and hence its hydrophilicity and tendency to wet, but at the same time provides chemical sites for derivatization.

Plasmas generated in the presence of reactive species (monomers) can polymerize, or react with the substrate, depositing a thin film on the surface. This process is referred to as plasma polymerization, or more formally as plasma-enhanced chemical vapour deposition, PECVD.<sup>6</sup> In this application a monomer is introduced into the plasma causing ionization, the ionized molecules can then polymerize with themselves to deposit a thin film. These films can be conformal providing properties that may differ from those of the substrate, Figure 5.

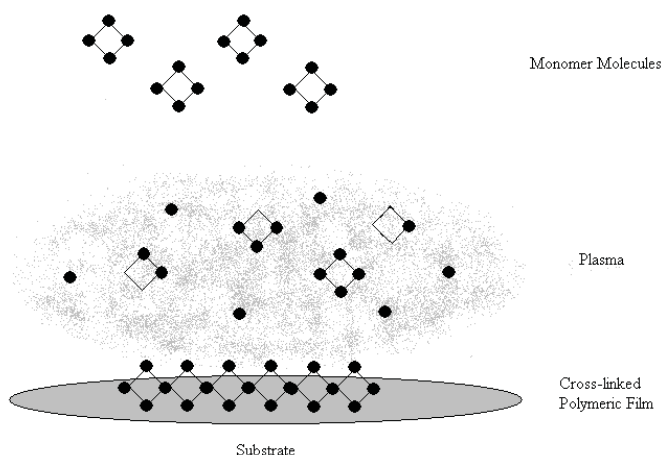


**Figure 5:** Plasma-enhanced chemical vapour deposition PECVD mechanism.

### 1.3 Sol-gel coatings

Another method to alter the surface chemistry of a substrate is to use a sol-gel coating. The term sol-gel refers to a chemical process by which a solution containing colloids (a sol) is transformed into a gel like phase containing a network of the colloidal particles and solvent. In this method, a thin film can be applied by dip-coating a substrate in a sol. Subsequent drying results in a coating on the surface. Precursors are often alkoxides of the form  $M(OR)_n$ , where R is an alkyl chain and M is an element such as Ti, or Si.<sup>11</sup>

The sol-gel is prepared by condensation and hydrolysis of the precursor in either acidic or basic conditions. The starting material is solvated in alcohol, and then under basic conditions hydrolysis replaces the alkoxide with hydroxyl groups. Condensation of hydroxyl ligands then produces a polymeric material composed of M-O-M and M- $\mu$ (OH)-M bonds.

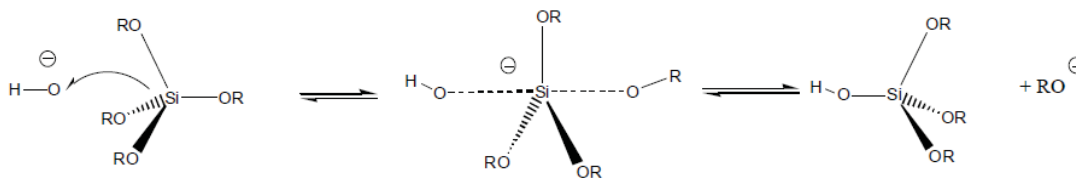


**Figure 6:** Base catalyzed hydrolysis of general silane,  $Si(OR)_4$ .

The use of long chain and fluorinated alkyl silanes as sol-gel pre-cursors has been reported to produce very low surface energy coatings on dipped substrates.<sup>12, 13</sup> The low surface energy results in a material with low affinity for water. Sol-gels were prepared from TEOS and 3,3,4,4,5,5,6,6,7,7,8,8,8-tridecafluorooctyltriethoxysilane (FAS, trade name Dynasylan), containing long fluorinated alkyl chains.

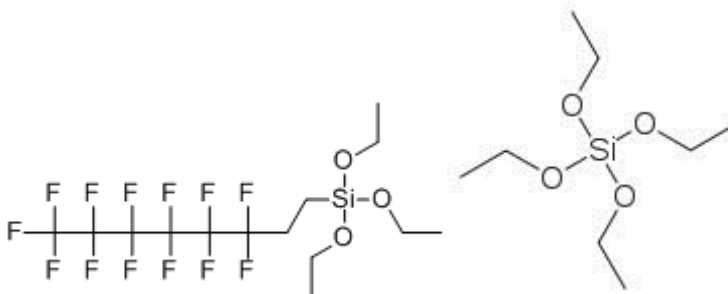


**Figure 7:** Sol-Gel precursors, (left) FAS, (right) tetraethyl orthosilicate.



## 2 Materials and methods

---

### 2.1 Electrospinning

Electrospinning solutions were prepared as follows: the polyurethane Desmopan, a thermoplastic polyurethane in pellet form purchased from Bayer, was dissolved in a solvent mixture of tetrahydrofuran/ dimethyl formamide, THF/DMF, with an optimum ratio of 60/40. Poly(vinylidene fluoride-co-hexafluoropropylene) (PVDF-co-HFP) pellets obtained from Sigma-Aldrich, were dissolved in a mixture of DMF/Acetone, with an optimum ration of 75/25. Solutions were made as a function of the polymer weight to solvent volume, typically in the range of 5-15% w/v, and stirred or shaken while sealed to prevent evaporation of solvent. Polymers were dissolved for a minimum of 3 hours by use of a magnetic stirrer or a shaker-table. Tetraethyl orthosilicate (TEOS), obtained from Sigma-Aldrich, was added to some of the solutions for electrospinning with no catalyst. Titanium dioxide nanoparticles were added to other polymer solutions. The solvents; DMF and THF were purchased from Burdick & Jackson Laboratories Inc., and dimethyl acetamide from Sigma Aldrich and were used without further purification.

Electrospinning was performed horizontally, with respect to the direction of the spinning axis, in an acrylic enclosure. Approximately 5 mL of solution was drawn up into a 30 mL glass Hamilton Company syringe, via the needle and tubing extension, 0.156 inch ID PFA tubing. The needles used were 20 gauge, 1 inch long stainless steel with a flat tip. The syringe was clamped into a syringe pump, Cole Parmer Instrument Company, Model # 75900-00, for maintaining a constant solution flow to the needle tip that was clamped into a port in the acrylic enclosure. Flow rates were varied from 10-100  $\mu\text{L}/\text{min}$ . The positive lead, from a Gamma High Voltage Research power supply, was connected to the needle tip via an alligator clip. A voltage between 10 and 20 kV was applied to the needle and was adjusted slightly to achieve 'smooth' electrospinning. Higher voltages tended to cause sputtering and erratic motion of the jet at the needle tip. Lower voltages resulted in thicker fibres. The collector used was a circular 15 cm diameter aluminum plate, mounted at a 20-35 cm working distance from the needle tip, and either connected to ground or to a negative terminal of the power supply. Non-stick aluminum foil, Alcan, was wrapped on the collector plate in order to facilitate removal of electrospun materials.

### 2.2 Plasma treatment

Plasma etching and treatment was carried out using a Flareon Series FLR-300TT Table Top Pulsed Plasma coating system (Plasmionique) which generates plasma using an inductively coupled power source (rf power 13.56 MHz, max 300W). The chamber was a 150 mm diameter by 150 mm tall vertical stainless steel cylinder with a 2.5 L volume; substrates are mounted on a 100 mm diameter steel plate. The matching circuit, two mass flow controllers, RF source and chamber were all contained within the installed unit. Argon was used as the flow gas; a water circulation/refrigeration unit provided cooling of the RF source. Control of parameters and data logging were performed in a specially designed Labview program. PECVD was attempted with hexamethyldisiloxane (Sigma-Aldrich).

Plasma treatment was performed by placing the substrate on the sample holder; in the case of very light samples that may be swept away by the vacuum, a small nut was used like a

paper-weight at its edge. All instrument settings were controlled through the plasma coater's software. The chamber was first pumped down to a pressure of 300 mTorr or better and then argon was introduced to the chamber via a mass flow controller, MFC, at a flow rate of between 1-10 sccm. The program contains a function to automatically modify flow to maintain a set vacuum; this was enabled by inputting the desired vacuum (e.g., 300 mTorr) and enabling the "PID" function. The power for the plasma source was set to 100 W, continuous mode, and run for a duration of five minutes. Successful ignition of plasma was observed with a characteristic violet light emission for argon. Once the experiment was completed, the pump was isolated with a valve to prevent back-flow, and turned off. The argon tank and MCF were closed and the substrate removed from the chamber after venting to atmospheric pressure.

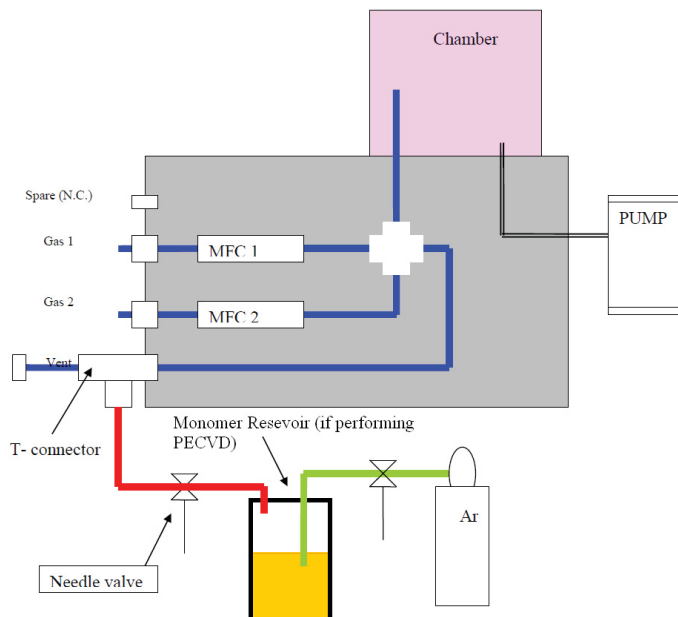


**Figure 8:** Plasma reactor schematic for PECVD, for plasma treatment no monomer reservoir is used.

## 2.3 Sol-gel coatings

Sol-gel experiments were carried out according to a published method,<sup>13</sup> where the sol was prepared using a 1:10 FAS:TEOS ratio by adding 0.859 mL of FAS, 3,3,4,4,5,5,6,6,7,7,8,8,8-tridecafluorooctyltriethoxysilane, supplied by Degussa with trade name Dynasylan F8261, to 5 mL of tetraethyl orthosilicate, TEOS, in 25 mL ethanol. This solution was mixed with a basic ethanol solution, made up of 6 mL 28% ammonium hydroxide, Burdick & Jackson Laboratories Inc., in 25 mL ethanol, and stirred for minimum of 12 hours. The sol-gel solution was sonicated for thirty minutes prior to use and samples were coated by dipping in the sol. Excess solution was blotted with a Kim wipe, and the sample was dried at room temperature followed by heating in a standard oven at 110 °C for a minimum of one hour. Electrospun materials to be coated were left on the aluminum foil on which they were collected in order to maintain the shape. Electrospun mats that were removed from the aluminum foil support and dipped into the sol-gel solution tended to collapse irreversibly into a hard clump, due to residual strain in the elastomeric polyurethane.

## **2.4 SEM imaging**

Sample morphology and fibre size were studied using a scanning electron microscope, Hitachi S-3700N. The variable pressure feature was used in order to prevent surface charging or the need to carbon or gold sputter-coat the samples. The instrument was typically operated at an accelerating voltage of 5-10 kV, a pressure of 10-50 Pa, and an emission current of 70-95  $\mu\text{A}$ . The instrument was also outfitted for energy-dispersive X-ray spectroscopy, EDX, which was used for elemental analysis and mapping. Quantification of the atomic composition of an electrospun fibre was performed by averaging the results of measurements from a minimum of five randomly selected different fibres.

## **2.5 ATR FTIR spectroscopy**

The surface chemistry and chemical bonding of the materials were analysed using a Fourier Transform Infrared, FTIR, spectroscopy microscope equipped with an attenuated total reflection cell, ATR-FTIR. The ATR cell consisted of a half-sphere germanium ATR crystal for contact with the sample surface, and a driving screw to establish thin contact. The penetration depth of infrared radiation into material using the Ge crystal is on the order of 0.3  $\mu\text{m}$ . This accessory required no sample preparation, thereby ensuring the morphology was not artificially altered. Infrared spectra were recorded over a frequency range of 675-4000  $\text{cm}^{-1}$ .

## **2.6 Contact angles**

To assess hydrophobicity 5  $\mu\text{L}$  water drops were placed on the sample and static contact and tilt angles were measured using a Digital Microscope (Keyence, VHX-600). Static contact angles were measured using the microscope's built-in rectangular mount and the microscope's built-in software. Contact angles were reported as an average of five measurements made per drop and five drops per surface, in order to minimize uncertainty based on surface variations and in defining the tangent of the drop at the three phase boundary. Tilt angles were measured by mounting the sample on a two-axis vice and then tilting the sample from horizontal until the drop began to roll. Tilt angles were reported as an average for a minimum of five drops, and one measurement each.

### 3 Results and discussion

#### 3.1 Fabrication by electrospinning

Polyurethane solutions with and without tetraethyl orthosilicate were electrospun as thin white mats, consisting of tangled webs of fibres, with nano- and micron-sized diameters. A 60/40 V/V THF/DMF solvent ratio was found to be optimal offering good solubility and volatility allowing the solution to be spun without drying and clogging at the tip, while evaporating sufficiently to give thin, dry fibres at the collector. Insufficient evaporation resulted in collection of wet fibres, which fused together due to residual solvent, and decreased the roughness profile. The solution was also in a good range of conductivity and surface tension, as the spinning was maintained at a steady rate at the tip, without erratic sputtering or axis-symmetric movement (rotation of the jet about the needle tip). Scanning electron microscopy was used to confirm the deposition of non-fused, evenly laid polyurethane fibres with a diameter range of roughly 0.75-2  $\mu\text{m}$ , with a mean value of  $1.4 \pm 0.38 \mu\text{m}$ , Figure 9.

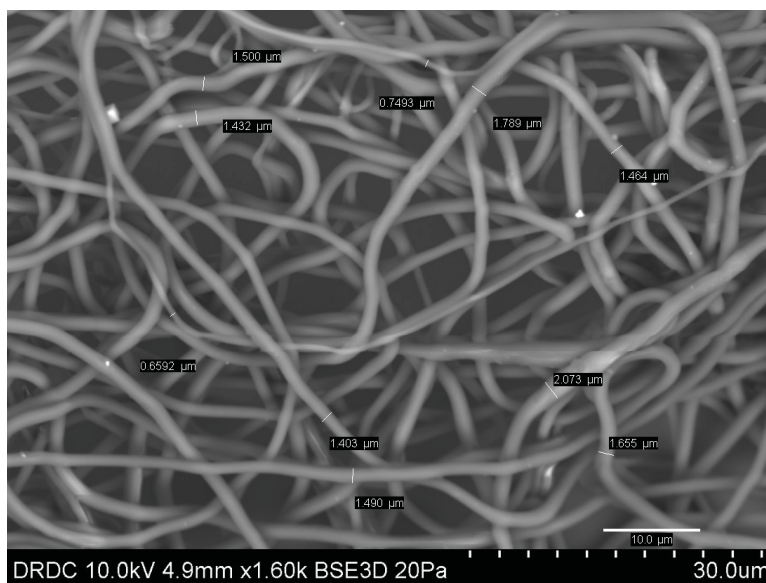


**Figure 9:** Electrospun mat from a solution containing 12% PU and 2% TEOS w/v in 60/40 THF/DMF, 35 cm working distance, 30  $\mu\text{L}/\text{min}$  flow rate, 20 gauge needle, 16 kV : grounded +/- applied field.

PVDF-co-HFP with and without TEOS was electrospun using the same apparatus and similar conditions to that of the polyurethanes. The solution was spun from a 75/25 DMF/Acetone mixture. The collected mat morphology was composed of very fine fibres (roughly 0.2-1.4  $\mu\text{m}$  diameter) with a mean diameter of  $0.6 \pm 0.40 \mu\text{m}$ , with some spherical and oval beads (2-4  $\mu\text{m}$  diameter), Figure 10.

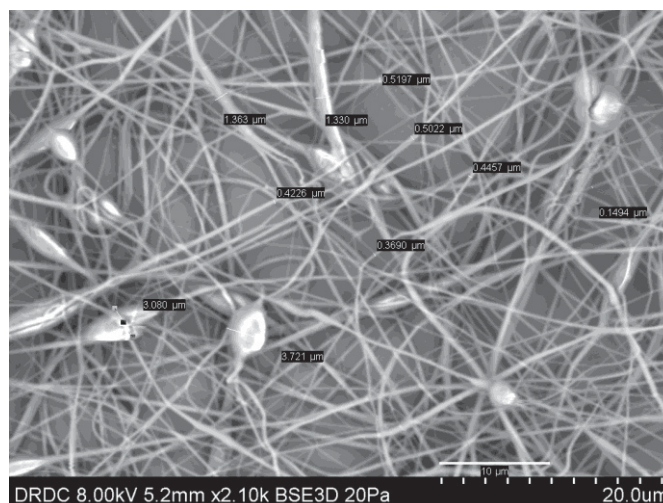


**Figure 10:** Electrospun mat from a solution containing 15% PVDF-co-HFP and 2% TEOS w/v in 75/25 DMF/acetone, 35 cm working distance, 30  $\mu\text{L}/\text{min}$  flow rate, 20 gauge needle, 20 kV : 10kV  $\pm$  - applied field.

The fibre diameter is a function of a number of the variables in the electrospinning process. First, the size of the drop formed at the end of a syringe is dependent of the surface tension of the polymer solution.<sup>14</sup> The lower the polymer solution surface tension is, the lower the voltage required to form the Taylor cone will be. The size of the jet expelled from the Taylor cone is proportional the size of the Taylor cone; a smaller Taylor cone produces finer fibres. Smaller fibre diameters have been obtained by the use of low surface tension solvents for cellulose acetate polymers spun from dimethyl acetamide and increasing amounts of acetone.<sup>15</sup> Once a jet is formed, then the stability of the jet, as a continuous stream of solution, depends on the polymer chains being entangled which is dependent on the polymer's molecular weight and concentration and is directly related to the solution viscosity. The average molecular weights of the polyurethane and polyvinylidene co-hexafluoropropylene used in this work are approximately 250,000 and 400,000 respectively. On average the PVDF-co-HFP solutions with the larger molecular weights resulted in thinner fibres than the polyurethane solutions.

The solution's conductivity, solvent evaporation rate, and the potential gradient between syringe tip and collector will determine how the jet travels and thins, during its flight to the collector. Given that a very fine jet is expelled, the conductivity of the solution and/or the potential field applied must be sufficiently high to cause the jet to undergo instabilities which result in it whipping around and thinning further as it is stretched and the solvent evaporates.<sup>16</sup> Increasing the solution conductivity by adding salt has been shown to decrease the fibre diameter.<sup>16</sup> It is thought that the instabilities are hierarchical, and therefore certain minimum voltages must be exceeded to 'access' the highest, thinning forces.

The mechanism of bead formation is not clearly understood, but is thought to be a result of surface tension and charge; other factors such as viscosity, vapour pressure and polymer concentration are pertinent. As a jet travels it undergoes a whipping transition where the jet is thinned and elongated. A consequence of the thinning is an increase in surface area, based on simple geometry. An increase in the surface area may in turn decrease the charge density on the jet's surface, resulting in a condition where the repulsive forces become smaller than the surface



tension. This force imbalance would then result in the minimization of the surface free energy by a contraction of the liquid into a spherical shape and hence bead formation. Solvent evaporation subsequently locks in the shapes of the beads and fibres. A high occurrence of beads has been reported to result from low polymer concentration, and that solutions with increased polymer concentration yield thicker, more uniform non-beaded fibres.<sup>17</sup> In the experiments presented here, beading was observed to occur in solutions up to about 9% wt/v of polyurethane and around 15-20% wt/v of poly vinylidene co-hexafluoropropylene. Beading was also observed to be a function of syringe flow rates. Decreasing the flow rate from 50 to 25  $\mu\text{L}/\text{min}$  during the electrospinning of 9.5 % polyurethane in 60/40 THF/DMF resulted in finer fibres, but a significant occurrence of beads, Figure 11.

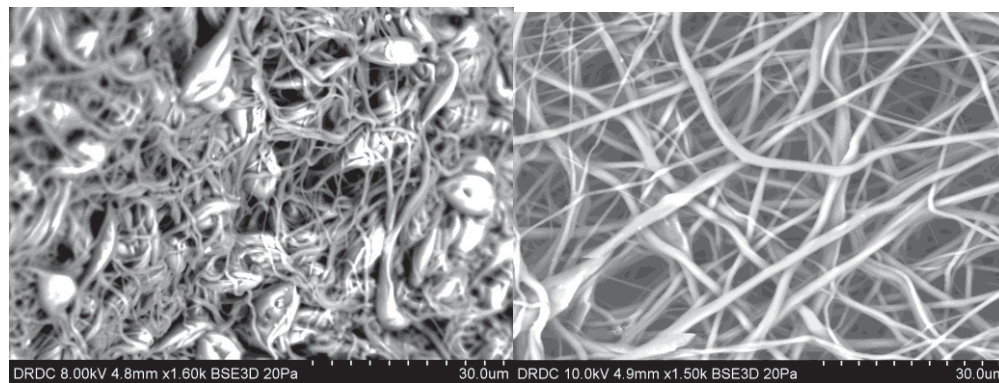


**Figure 11:** Effect of flow rate for electrospun 9.5% polyurethane in 60/40 THF/DMF. (left) 25  $\mu\text{L}/\text{min}$ , (right) 50  $\mu\text{L}/\text{min}$ , at a working distance of 35 cm, 20 gauge needle, 13 kV : 10kV +/- applied field.

The effect of beads on a mat's properties has been debated in the literature. Some reports indicate that bead formation enhances a material's hydrophobicity by giving it a second, nano-scale roughness,<sup>18</sup> while others argue that, while providing a second layer of roughness, it is not hierarchical, and is randomly found along the fibres, therefore their presence should be considered a defect.<sup>19</sup> Another study concluded that for water repellency, thin beaded fibres were superior to thicker non-beaded fibres if the bead density was sufficiently high and the bead size was small.<sup>20</sup> In cases where the beads are too large, or scarce, lower contact angles were observed. These conditions seem to indicate that beads contribute positively to hydrophobicity when in the low-micrometer scale, thereby adding to the roughness, and once exceeding the low-micrometer size range they contribute negatively by mimicking a flat, non-roughened surface, and provide larger contact area. To minimize beading, solutions should be more concentrated, however this results in larger fibres, and therefore the solution concentration is a compromise that attempts to minimize beading and fibre diameter. Ultimately the fibre morphology depends on the polymer solution's surface tension, viscosity, and charge, along with experimental parameters such as voltage and flow rate. These need to be tailored for producing fibre mats with the required properties.<sup>21</sup> There is no visible evidence, on the scale imaged, in Figures 9 and 10, of silica nanoparticles from the TEOS added to the electrospinning solutions.

## 3.2 Roughness and derivatization

### 3.2.1 Microphase separation of electrospun polymer blends

A solution of 10% polyurethane and 4% PVDF-co-HFP was electrospun with the aim of seeing if the fluorinated polymer would have an effect on the resultant fibre structure. Fibres electrospun from this solution were observed by SEM, under variable pressure, to have some nodules at the surface, Figure 12. These nodules and some regions of the polymer fibres were lighter which may indicate charging. The fluorinated polymer is expected to charge to a greater degree than the polyurethane due to the presence of hydrophilic groups in the latter. Further experimentation is required to optimize the benefits of this organization.

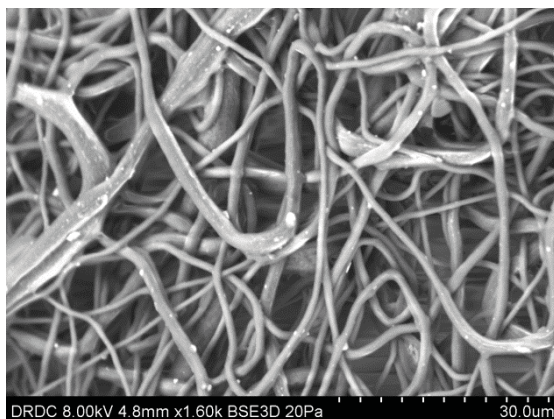


*Figure 12: SEM image of electrospun 10% polyurethane with 4% PVDF-co-HFP. The fibres appear to be rough with white nodules.*

### 3.2.2 Electrospinning with nanoparticles

One requirement for superhydrophobicity is to have a rough surface on the micrometer and nanometer scales. The micron scale roughness is provided by the fibres of electrospun mats. Secondary roughness on the nano-scale could be provided by inclusion of nano-particles in the electrospinning solution. Development of additional roughness was attempted by adding  $\text{TiO}_2$  particles (1% by weight) to a solution of polyurethane and then electrospinning. A SEM image of the resultant fibres is presented in Figure 13. The  $\text{TiO}_2$  particles are visible as small clusters on the surface of the fibres. The areal density of these particle clusters is low, and experimentation is required at higher loading and for smaller particles. It is also expected that these particles will be hydrophilic and require derivatization in order for them to be hydrophobic or oleophobic. Further investigation is required to fully explore the effects of particle loading and chemical derivatization, on the surface properties of nanoparticle modified materials.

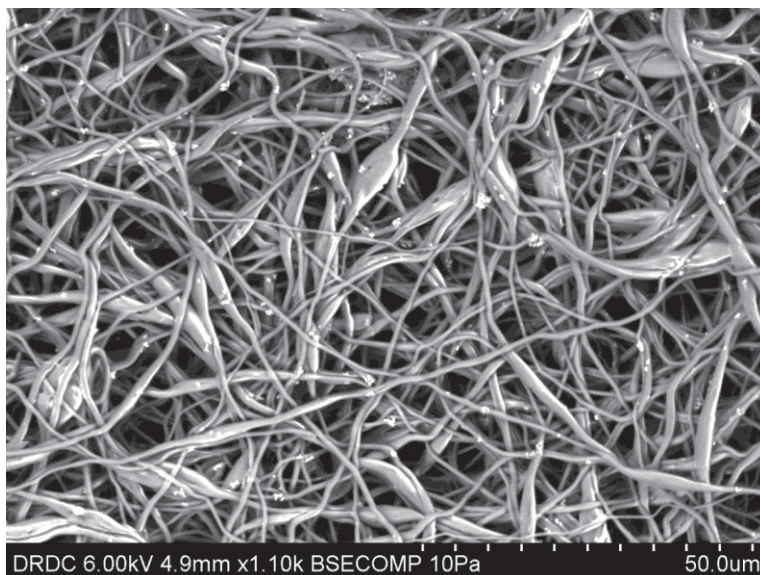


**Figure 13:** SEM image of electrospun polyurethane with 1%  $\text{TiO}_2$ .  $\text{TiO}_2$  particles are visible as white particulate clusters on the fibre surface.

### 3.2.3 Effect of TEOS addition to electrospinning solutions

Tetraethyl orthosilicate (TEOS) was added to electrospinning solutions and was expected to react with terminal alcohol groups in the polyurethane, arising from the diol building block, to form bonded silica particles or at least a larger functional site for chemical derivatization, Figure 14. There was also the potential that the TEOS would react with several polymer chains, resulting in cross linking, increased chain length and potentially increased fibre strength. As a control TEOS was also added to the PVDF-co-HFP solution, which does not have functional groups available for the TEOS to bond with.

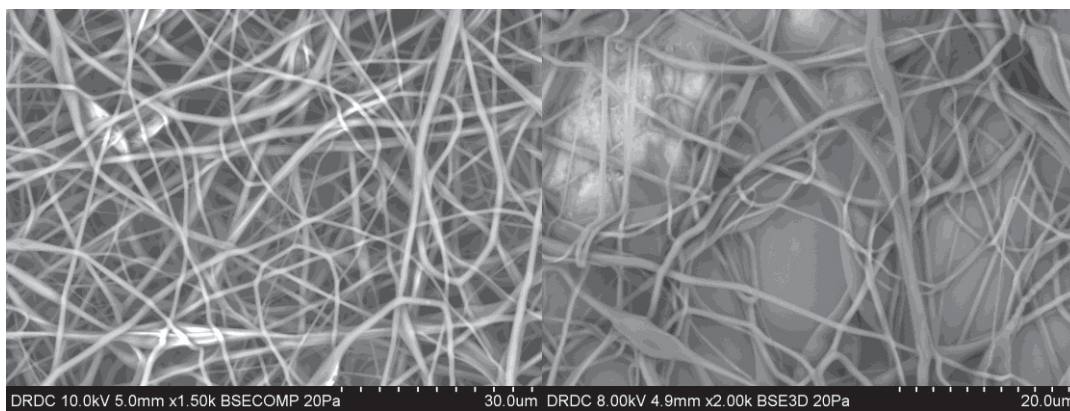


**Figure 14:** Left, 9.5% polyurethane, and right 10% polyurethane + 4% TEOS electrospun fibres from 60/40 THF/DMF, 35 cm working distance, 20 gauge needle, 15-20 kV +, 10 kV - collector, 25-30  $\mu\text{L}/\text{min}$  flow rate.



SEM images of fibres spun from solutions containing polyurethane, and polyurethane plus TEOS appeared similar though perhaps with finer diameter fibres being produced, Figure 14. A new minimum fibre diameter of 0.15  $\mu\text{m}$ , was measured compared to 0.66  $\mu\text{m}$  measured for polyurethane by itself. This may be a consequence of the TEOS solution having lower surface tension. TEOS has a surface tension of 23.5 dyne/cm while THF and DMF are 26.4 and 37.1 dyne/cm at 20 °C respectively. The contact angles for fibre mats prepared with TEOS were not statistically different from contact angles measured for straight polyurethane mats;  $131.0^\circ \pm 3.0^\circ$  for polyurethane-TEOS compared to  $127.6^\circ \pm 5.1^\circ$  for straight polyurethane.

### 3.2.4 FTIR spectroscopy of electrospun fibres

ATR-FTIR spectra were taken of stock polyurethane and PVDF-co-HFP, and of electrospun fibre mats of these polymers from solutions containing the polymers and TEOS. ATR-FTIR is a spectroscopic technique that provides information on the types of bonds present in the surface. Figure 15 presents the spectra recorded of a polyurethane pellet and of an electrospun mat from a solution of the polyurethane and 2% TEOS. The main differences between the two spectra are the loss of the broad peak around 3400-3700  $\text{cm}^{-1}$ , and a reduction in the size of the sharp peak at about 3300  $\text{cm}^{-1}$ , associated with  $-\text{OH}$  and  $-\text{NH}-$  groups of the polyurethane, respectively. In addition absorptions from Si-O-Si at 792, 1010, 1074 and 1254  $\text{cm}^{-1}$  are present for the polyurethane + TEOS material. These results indicate the reaction of TEOS with the alcohol groups and the presence of silicate in the material. There may be interactions of the silicates with other chemical groups in the polyurethane such as  $-\text{NH}-$ .

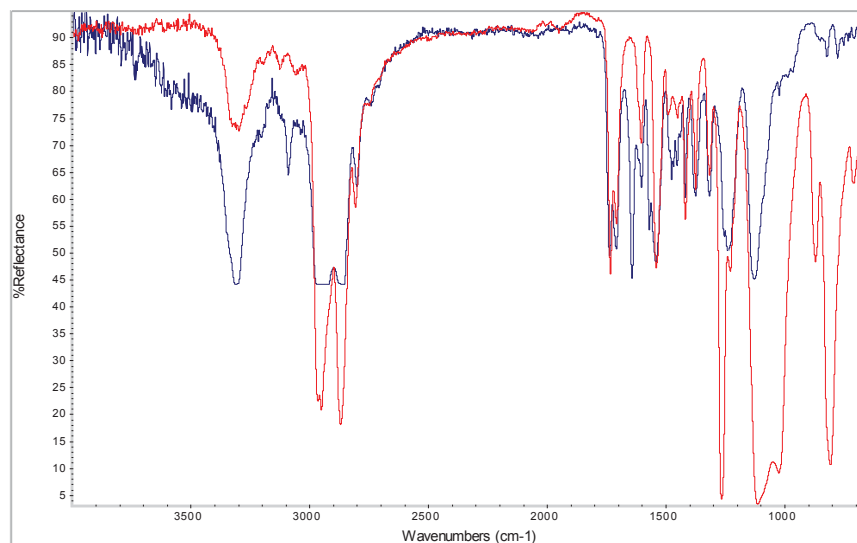


**Figure 15:** FTIR Spectra: polyurethane pellet (blue line) and an electrospun mat from a solution of 12% Polyurethane + 2% TEOS (red line).

The ATR-FTIR spectra of PVDF-co-HFP, and of fibres electrospun with TEOS, also show the presence of silicate linkages, Figure 16. In this case the polymer contains no hydroxyl or other functional groups with which the TEOS can react, and so the silicates are not chemically bonded to the polymer. As a consequence silicate growth may proceed by a different mechanism, and may organize differently than silicates in the polyurethane materials.

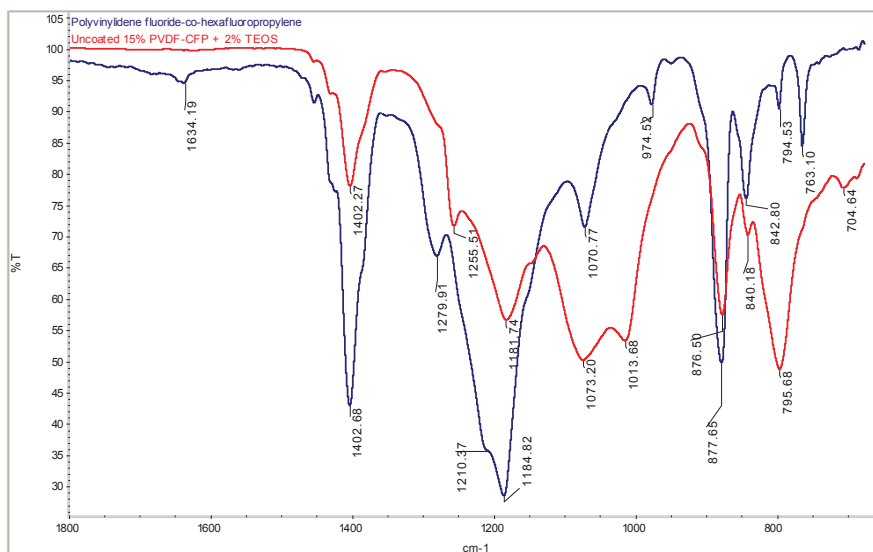


**Figure 16:** FTIR Spectra: PVDF-co-HFP pellet (blue line) and a mat electrospun from a solution of 15% PVDF-co-HFP + 2% TEOS (red line).

### 3.3 Sol-gel coatings

In order to decrease the surface energy of the fibre mats and increase the contact angle, fibre mats of polyurethane and PVDF-co-HFP, were dipped into a sol-gel solution. The solution contained the fluorinated silane, 3,3,4,4,5,5,6,6,7,7,8,8,8-tridecafluorooctyltriethoxysilane, FAS, in a 1:10 molar ratio to TEOS, prepared using hydrolysis in ethanol under basic conditions.<sup>12</sup> SEM imaging of a sol-gel coated polyurethane + TEOS mat revealed an rough distribution over the fibres' surface, giving the fibres an additional nano-texture due to the very small size of the deposited silica particles, Figure 17. Fibre mats coated in this manner exhibited larger water contact angles, presumably due to the very low surface energy of the fluorinated silica particles and improved multiscale roughness due to the nano-texturing from the silica particles. Fibre mats prepared from PVDF-co-HFP + TEOS and dipped into the sol-gel solution resulted in the formation of a highly caked sol-gel coating, Figure 18. The difference between the two sol-gel coated electrospun fibre mats containing silica particles is unclear, though it was found that pure PVDF-co-HFP electrospun fibres also resulted in an extensive deposition of caked on silica.

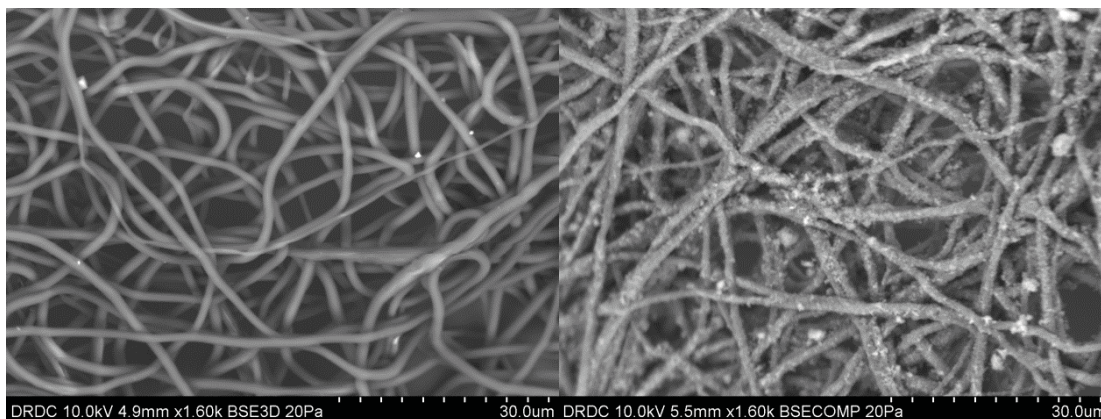


**Figure 17:** *Electrospun polyurethane + TEOS, before and after coating in 1:10 FAS:TEOS sol-gel.*

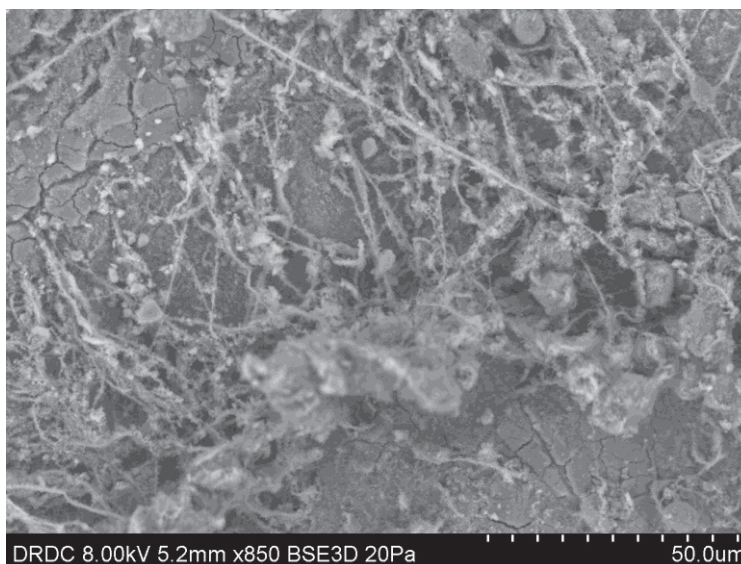


**Figure 18:** *Electrospun PVDF-co-HFP + TEOS mat coated in 1:10 FAS:TEOS sol-gel. Compare to Figure 10 of an uncoated PVDF-co-HFP + TEOS mat.*

The difference in sol-gel coating formation on the polyurethane and PVDF-co-HFP based fibres may be due to the ability, or lack thereof, of the alkyl siloxanes to chemically bond to the polymer chain. Polyurethane fibres electrospun with TEOS are expected to have a uniform distribution of silicate throughout the material due to nucleation sites at the terminal hydroxyl groups. Thus only a portion of the silicate is available for reaction with the sol, and the size of the existing silicate particles may be small. PVDF-co-HFP on the other hand, has no such nucleation sites to react with TEOS. EDX measurements of the polymer + TEOS fibres indicated the presence of Si and O in both polymer fibres and more of these elements in PVDF-co-HFP than the polyurethane, Table 1. More research is required to clarify the mechanism behind the sol-gel formation.

### 3.3.1 FTIR spectroscopy of sol-gel coated polymer fibres

After the fibres were coated with the sol-gel and dried, ATR-FTIR spectra were taken and presented with the spectra for the polyurethane and PVF-co-HFP polymers, Figure 19 and 20 respectively. In the spectrum of polyurethane + TEOS the resonances from the polyurethane are still visible in the 1800-1300  $\text{cm}^{-1}$  region, blue line in Figure 19. After the material was coated with the sol-gel, these resonances were not observed and the spectrum was dominated by a large Si-O-Si silicate resonance at 1050  $\text{cm}^{-1}$ , red line in Figure 19. Resonances due to C-F bonds are observed from 1141-1189  $\text{cm}^{-1}$ .

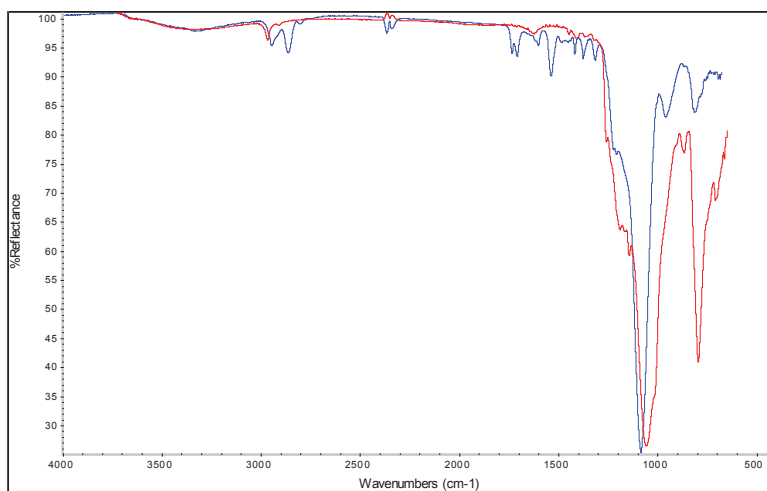


**Figure 19:** ATR-FT-IR Spectra: FAS-coated 12% Polyurethane + 2% TEOS, red line; and Uncoated 12% Polyurethane + 2% TEOS, blue line.

Similar observations are made for the spectra of PVDF-co-HFP + TEOS before and after sol-gel coating, Figure 20. Resonances observed for the PVDF-co-HFP in the 1800-1300  $\text{cm}^{-1}$  frequency region, red line, are not observed after the material is coated with the sol-gel. The spectrum of the sol-gel coated polymer is dominated by the Si-O-Si peaks at 1050  $\text{cm}^{-1}$ .

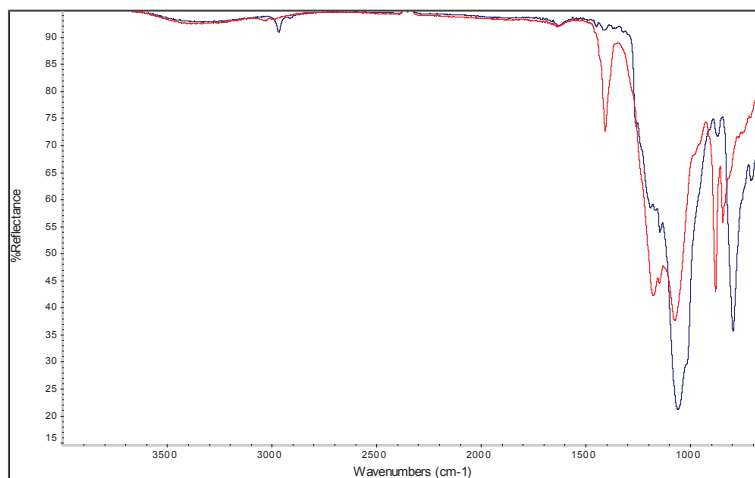


**Figure 20:** ATR-FT-IR Spectra of 15% PVDF-co-HFP + 2% TEOS, red line, and sol-gel coated 15% PVDF-co-HFP + 2% TEOS, blue line.

### 3.3.2 Energy dispersive X-ray analysis of polymer and sol-gel coatings

Energy dispersive X-ray analysis, EDX, was conducted on the electrospun polymers + TEOS and sol-gel coated polymers + TEOS, and the results are presented in Table 1. Note that conditions under which the EDX spectra were recorded may not have been constant from sample to sample, and therefore the results are considered as indicative only. The electron beam of the SEM was focussed onto fibres for these measurements. For uncoated polyurethane + TEOS, there was no fluorine observed and about 4.4 % silicon. In comparison the PVDF-co-HFP + TEOS material contained about 6.5 % fluorine and about 19 % silicon. These results are consistent with TEOS forming silicate in the polymer fibres and the presence of fluorine in PVDF-co-HFP. After sol-gel coating the polyurethane + TEOS material, the fluorine, oxygen and silicon content appears to have increased consistent with the presence of sol-gel from TEOS and FAS.

**Table 1:** *Composition of polyurethane and PVDF-co-HFP, electrospun with TEOS, before and after coating with FAS sol-gel as measured by EDX.*

Element	12% Polyurethane + 2% TEOS		15% PVDF-co-HFP + 2% TEOS	
Atomic %	Uncoated	Coated	Uncoated	Coated
Carbon	79.6±7.0	60.6±4.4	43.6±1.6	65.7±3.7
Oxygen	15.0±4.2	28.1±2.4	24.9±3.3	9.2±2.3
Fluorine	0.0±0.0	3.1±0.5	6.5±0.9	22.0±1.0
Silicon	4.4±3.0	7.6±2.2	18.6±3.5	2.4±0.7
Other	1.1±0.2	0.6±0.1	6.4±5.5	0.6±0.1

For the PVDF-co-HFP + TEOS fibres, sol-gel coating resulted in an increase in fluorine, though the oxygen and silicon content appears to have decreased. The increase in fluorine content is consistent with reaction of FAS with the polymer-silicate, while the decrease in oxygen and silicon content indicates that the sol-gel reaction is predominantly depositing FAS in preference to TEOS. As seen in SEM imaging in Figure 18, the sol-gel coating was not evenly deposited on the fibres, but formed a caked material between the fibres. The EDX measurements reported here were performed on five different fibres, and the caked portions were not included in the results in Table 1. The caked layer was independently measured and determined to be composed of roughly 33:40:14:13 atomic % C:O:F:Si, indicating dried portions of solid sol-gel. Unlike the polyurethane coating that contains Si-O-Si as well as fluorinated alkyl chains at the surface, it appears the coating of the PVDF-co-HFP fibres resulted in a surface composed of the fluoro-alkyl chains. Further investigation is required.

### 3.3.3 Contact angle measurements

Sol-gel coating was noted to markedly improve the hydrophobicity of polyurethane + TEOS and PVDF-co-HFP + TEOS polymer mats, Figures 21 and 22, and Table 2.



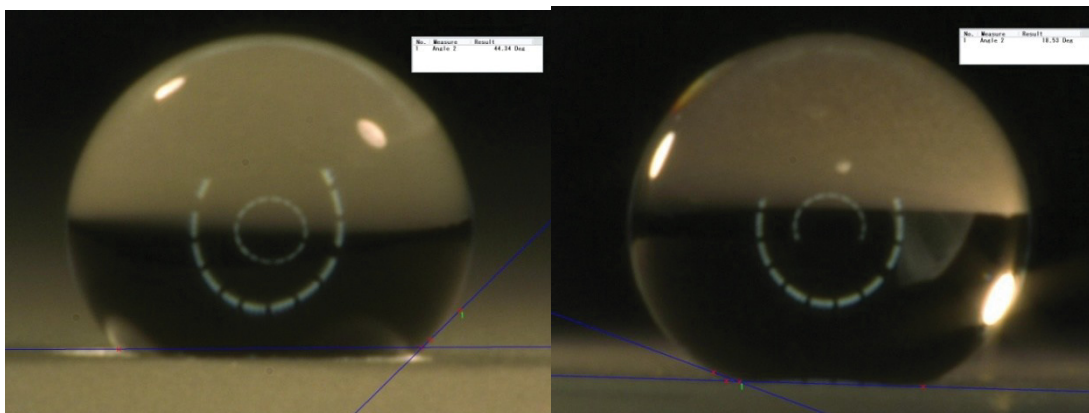


**Figure 21:** A 5  $\mu\text{L}$  water drop on electrospun polyurethane + TEOS before coating, left, and after coating with the sol-gel, right. The contact angles are  $131^\circ$  and  $162^\circ$  respectively.

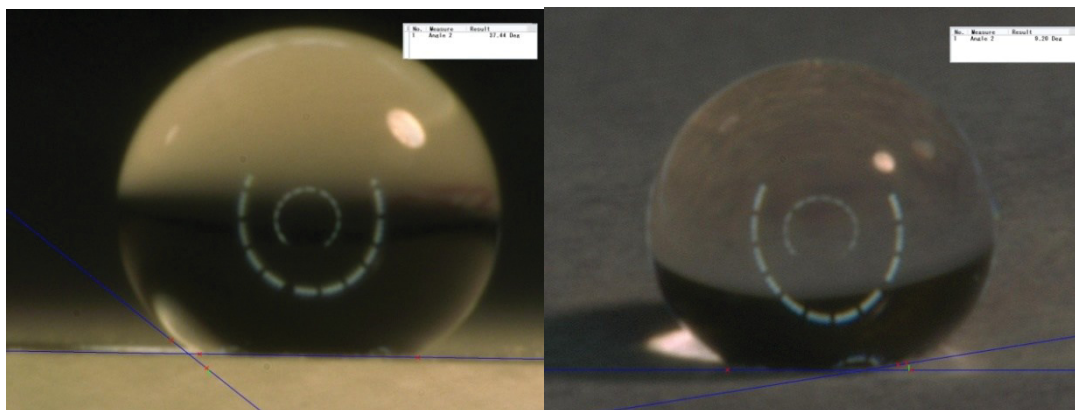


**Figure 22:** A 5  $\mu\text{L}$  water drop on electrospun PVDF-co-HFP + TEOS before coating, left, and after coating with the sol-gel, right. The contact angles are  $134^\circ$  and  $170^\circ$  respectively.

**Table 2:** Contact angle measurements for polymers before and after sol-gel coating.

Sample	Static Contact Angle 5 $\mu\text{L}$ drop H <sub>2</sub> O	Tilt Angle 5 $\mu\text{L}$ drop H <sub>2</sub> O
12% Polyurethane + 2% TEOS uncoated	$131.0^\circ \pm 3.0^\circ$	*
12% Polyurethane + 2% TEOS Coated	$162.6^\circ \pm 2.1^\circ$	$1.5^\circ \pm 2.0^\circ$
15% PVDF-co-HFP + 2% TEOS uncoated	$134.5^\circ \pm 1.9^\circ$	*
15% PVDF-co-HFP + 2% TEOS coated	$\sim 170^\circ$ **	$4.0^\circ \pm 4.9^\circ$ ***

\* drop pinned (would not roll or slide at  $90^\circ$ ).

\*\* drop rolled when placed on the surface.

\*\*\* upon drop resting after being placed.

Contact angles measured for mats composed of polyurethane and TEOS were typically in the range of 120-135°, and therefore hydrophobic due to the roughness imparted by electrospinning. Sol-gel coating increased the water repellency to superhydrophobic ranges, achieving contact angles of  $162.6 \pm 2.1^\circ$ , Table 2. Furthermore, the coating prevented water drops from pinning to the surface and the average tilt angle was  $1.5 \pm 2.0^\circ$ , with some drops rolling off the surface instantaneously (these are recorded as 0°). The extremely low tilt angle indicates the water droplet rests in the Cassie-Baxter state. In addition water drops were observed to bounce off of these mats and the adhesive forces between the water and the syringe were greater than between the water and surface, often making it difficult to place a drop on the surface.

Fibre mats composed of PVDF-co-HFP + TEOS were quite hydrophobic, with water contact angles of  $134.5 \pm 1.9^\circ$ . The higher angle compared to polyurethane - TEOS was likely a combination of lower surface energy and increased surface area. The low surface energy of PVDF-co-HFP arises from the high fluorine content of the polymer backbone. As expected, sol-gel treatment of PVDF-co-HFP + TEOS resulted in very high contact angles and very low tilt angles. For this reason the static contact angle is not measured, as a drop did not rest on the surface unless it encountered a physical well or a higher energy portion of the coating. The recorded tilt angle,  $4.0 \pm 4.9^\circ$ , is also based on drops that find a resting place on the mat.

The difference in the surface structures and chemistries of the sol-gel coated surfaces is interesting and needs to be studied further in order to determine if this behaviour is driven by the chemistry of the polymers or by some other mechanism. Long term durability, prolonged water-surface contact, and organic liquid-surface interactions also need to be studied. Nonetheless, the ability of the sol-gel to coat and thus enhance hydrophobicity of electrospun fibres has been demonstrated.

### 3.4 Plasma treatment

In this final section the effects of plasma treatment on both types of electrospun polymers are considered. Treatment with argon plasma in a low-vacuum cold chamber was found to render both polymer substrates hydrophilic with a 100W power treatment as short as four minutes. When performing contact angle measurements, water drops would instantly collapse and wet into the surface, therefore exhibiting contact angles that were practically 0°. The plasma exposure time required to reach maximum wetting decreased with increasing power.

In this work, ATR-FTIR spectra of both plasma treated polymers, showed no change from their untreated counterparts yet exhibit hydrophilicity. Hydrophilicity is believed to occur due to an increase in surface energy by the plasma, which generated free radicals on the fibre surface. It is surmised that upon exposure to the ambient air, the radicals react with oxygen, carbon dioxide and water vapour, producing oxygen containing functional groups such as hydroxyls and carbonyls. An ATR-FTIR and ESCA (electron spectroscopy for chemical analysis) study of the effects of nitrogen and argon plasma on a polyurethane surface indicated that the decomposition of -C(=O)O- bonds in the polyurethane were responsible for the increased wettability.<sup>22</sup> The ability of the pure PVDF-co-HFP polymer to transform from near-superhydrophobic to hydrophilic with argon plasma treatment suggests the first mechanism, as the polymer contains no ester groups to decompose. The decomposition mechanism has been supported by a study in which polyurethane samples were treated in an  $^{18}\text{O}_2$  plasma and aged in  $^{16}\text{O}_2$  and compared to

those prepped with  $^{16}\text{O}_2$  plasma and aged in  $^{18}\text{O}_2$ ; it concluded that the addition of the oxygen in the ageing step was negligible.<sup>23</sup> However, it is possible that using oxygen in the plasma saturated the surface's reactive sites, preventing further reaction upon exposure to air, where if argon had been used followed by labelled oxygen in the aging step then the reaction upon exposure in the ageing step might have been clearer. Further insight into the mechanism of plasma-induced wettability is required to understand its origin and how conditions can be optimally applied.

The increase in surface energy causes a strong attraction to water, resulting in contact angles that are practically  $0^\circ$ , as they instantly wick into and wet the surface upon contact. A benefit to these treatments is the relatively shallow depth of modification, which allows for reaction of the surface without altering the polymers bulk properties; the depth has been determined to be typically 50-500 Å.<sup>24</sup> The ability to modify a polymer's surface energy results in the ability to tune the surface properties.

Another means of tuning the surface properties is through plasma polymerization, where a monomer is introduced into plasma and allowed to react with the surface. Besides being able to perform polymerization in-line with treatment, another advantage is that no solvents or initiator are required for the polymerization process. It is reported that a significant number of monomers, even those without favourable polymer forming functionalities such as unsaturated bonds, can be polymerized in this process versus conventional chemical methods.<sup>25</sup>

Plasma polymerization was attempted by modifying the plasma reactor with a monomer reservoir, both bubbled in line with a process gas and as an isolated, terminal flask. When using the bubbler, the process gas, argon, was bubbled through the monomer to increase volatilization. When using the isolated terminal, volatilization was accomplished through introducing the monomer at low pressures (in the range of 50-500 mtorr) using an isolation valve. The monomer was introduced through the chamber vent to prevent condensation damage to the mass flow controllers ('MFC' in the schematic) in both set-ups. Polymerization was attempted using the monomer hexamethyldisiloxane (HMDSO),<sup>26</sup> however technical challenges in controlling the vacuum in a range suitable for maintaining the plasma and effecting polymerization limited the suitability of this approach. A modified plasma polymerization scheme to avoid these issues is presented in Figure 23. This will require further modification to the reactor, which, while well set-up for simple plasma treatment, lacks an input valve that correctly introduces monomer vapour. Ideally, the bubbler would be connected in-line with a gas, but after the mass flow controller, this would give the user fine control over the input flow rate of the gas using the MFC, the reduced flow would then bubble through the monomer at a controllable rate.



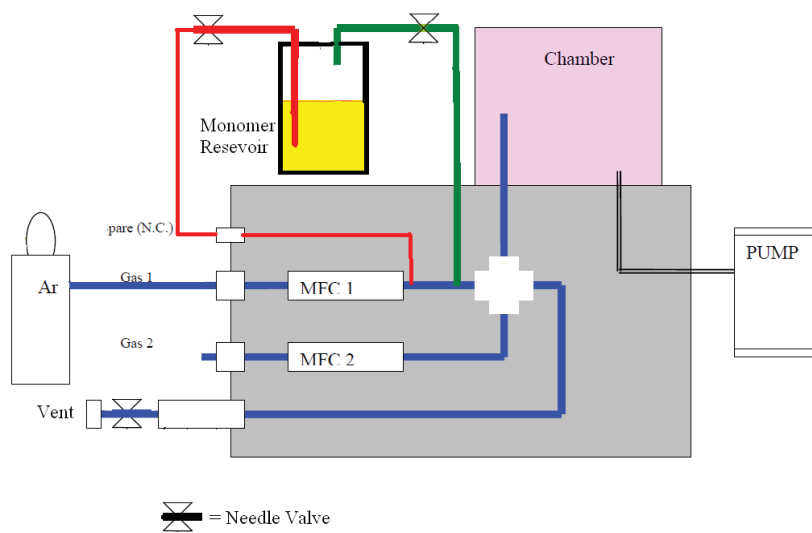


**Figure 23:** A modified PECVD set-up.

## 4 Conclusions and future work

---

In this study a number of methods for making superhydrophobic materials based on electrospun fibres have been explored. The electrospun fibres have diameters on the micron scale and the surface energy can be varied by appropriate selection of the polymers used. The fibre diameter can be controlled by the surface tension of the polymer solution used for electrospinning, and other experimental parameters. Polyurethane and polyvinylidene-co-hexafluoropropylene were both successfully electrospun and characterized as micro- to nano-scale fibres using scanning electron microscopy. Secondary roughness was achieved in the materials through several methods, including the formation of beaded fibres, addition of nanoparticles, phase separation of polymers with different surface energies, and sol-gel reactions. The contact angles measured for water drops on the fibre surfaces were around  $130^\circ$ , however, it was often found that the drops were pinned to the surface by fibres that had penetrated the drops and so they would not roll off of the surface.

Direct electrospinning of tetraethyl orthosilicate, TEOS, mixed with the polymer electrospinning solution, resulted in reduced fibre diameters due to the reduction in solution surface tensions, and the formation of silicates in the electrospun fibres. The presence of the silicates in the fibres was determined by ATR-FTIR and EDX spectroscopy. Sol-gel coatings employing fluorinated alkyl silanes were successfully used to add hydrophobic nanoparticles to the surface of the electrospun fibres. As a result water drops supported on these fibres had contact angles in excess of  $160^\circ$  and very small tilt angles were required before water drops ran off of the surface. These materials can be classified as superhydrophobic, supporting water drops in a Cassie-Baxter state.

Finally by treatment of surfaces with argon plasma it was possible to make the surfaces hydrophilic, so that water drops completely wetted the fibrous mats. Treatment of a surface in this manner could be used to functionalize a surface for further chemical derivatization in order to obtain the desired surface energy. In a similar manner, plasma polymerization was tried in order to modify the surface chemistry, however, finer control of the metering of the reactive monomer is required.

This work has demonstrated a number of methods for producing nano-scale roughness on electrospun fibres, methods for modifying the surface energy, and the production of highly water repellent surfaces. More work is required on each of the technologies discussed above to fully evaluate their potential and to optimize material durability. Some of the technologies can be directly applied to conventional coatings and in the modification of the surface properties of textiles. The technologies considered should also result in oleophobic, or oil repelling materials. Finally these technologies should be considered and test for their suitability for unique applications where high liquid repellency is an asset.

## References

---

- [1] Mimicking Nature: Physical basis and artificial synthesis of the Lotus-effect. S.C.S. Lai: Universiteit Leiden, **2003**.
- [2] Agarwal, S., Horst, S., Bognitzki, M. Electrospinning of Fluorinated Polymers: Formation of Superhydrophobic Surfaces. *Macromol. Mater. Eng.* **2006**, *291*, 592-601.
- [3] Ma, M., Gupta, M., Li, Z., Zhai, L., Gleason, K., Cohen, R., Ruber, M., Rutledge, G. Decorated Electrospun Fibres Exhibiting Superhydrophobicity. *Adv. Mater.* **2007**, *19*, 255-259.
- [4] R. Wenzel, *Resistance of solid surfaces to wetting by water*, Ind. Eng. Chem., 1936, 28, 988. A.B.D. Cassie and S. Baxter, *Wettability of porous surfaces*, Trans. Faraday Soc. 1944, 40, 546. Acatay, K., Simsek, E., Ow-Yang, C., Menciloglu, Y. Tunable, *Superhydrophobically stable polymeric surfaces by electrospinning*, *Angew. Chem. Int. Ed.* **2004**, *43*, 5210-5213.
- [5] Li, X.-M.; Reinhoudt, D.; Crego-Calama, M., *What do we need for a superhydrophobic surface? A review on the recent progress in the preparation of superhydrophobic surfaces*, Chem. Soc. Rev., **2007**, *36*, 1350–1368.
- [6] *Plasma Polymerized Coatings*; Midwest Tungsten Services: Willowbrook Illinois, <http://www.tungsten.com/tipspoly.pdf>, accessed June **2014**.
- [7] Arefi, F., Andre, V., Montazer-Rahmati, P., Amouroux, J. Plasma polymerization and surface treatment of polymers. *Pure and Applied Chem.* [Online] **1992**, *64*, 715-723.
- [8] Teo, W.E., Ramakrishna, S. A review on electrospinning design and nanofibre assemblies. *Nanotechnology.* **2006**, *17*, 14.
- [9] Conrads, H., Schmidt, M. Plasma generation and plasma sources. *Plasma Sources Sci. Technol.* [online] **2002**, *9*, 441-454.
- [10] Gurnett, D.A., Bhattacharjee, A. *Introduction to Plasma Physics: With Space and Laboratory Applications*. Cambridge, UK: Cambridge University Press, **2005**, p.2.
- [11] Brinker, C.J., Hurd, A.J. Fundamentals of sol-gel dip-coating. *J. Phys. 111 France.* **1994**, *4*, 1231-1242.
- [12] Wang, C., Li, M., Jiang, G., Fang, K., Tian, A. Surface Modification with Silicon Sol on Cotton Fabrics for water-repellant finishing. *RJTA.* **2007**, *11*, 27-34.
- [13] Wang, H., Fang, J., Cheng, T., Ding, J., Qu, L., Dai, L., Wang, X., Lin, T. One-step Coating of Fluoro-containing Silica Nanoparticles for Universal Generation of Surface Superhydrophobicity. *Chem. Comm.* Cambridge, U.K. **2008**, 877-879.

- [14] Fong, H., Reneker, D., Elastomeric nanofibres of styrene-butadiene-styrene triblock copolymer. *J. Polym. Sci: Part B Polym. Phys.* **1999**, *37*, 3488-93.
- [15] Liu, H., Hsieh, Y. Ultrafine fibrous cellulose membranes from electrospinning of cellulose acetate. *J. of Polymer. Sci Part B: Polymer Physics.* **2002**, *40*, 2119-29.
- [16] Reneker, D., Yarin, A., Fong, H., Koombhonge, S. Bending instability of electrically charged liquid jets of polymer solutions in electrospinning. *J. Appl. Phys.* **2000**, *87*, 4531-4547.
- [17] Zong, X., Kim, K., Fang, D., Ran, S., Hsiao, B., Chu, B. Structure and process relationship of electrospun bioabsorbable nanofibre membranes. *Polym. J.* **2002**, *43*, 4403-4412.
- [18] Li, X., Reinhouldt, D., Crego-Calama, M. What do we need for a superhydrophobic surface? A review on the recent progress in the preparation of superhydrophobic surfaces. *Chem. Soc. Rev.* **2007**, *36*, 1350-1368.
- [19] Liu, Y., He, J., Yu, J., Zeng, H. Controlling numbers and sizes of beads in electrospun nanofibres. *Polym. Int.* **2008**, *57*, 632-636.
- [20] Ma, M., Mao, Y., Gupta, M., Gleason, K., Rutledge, G. Superhydrophobic fabrics produced by electrospinning and chemical vapour deposition. *Macromol.* **2005**, *38*, 9742-9748.
- [21] Drew, C., Wang, X., Samuelson, L., Kumar, J. The effect of viscosity and filler on electrospun fibre morphology. *J. Macromol. Sci. Part A Pure Appl. Chem.* **2003**, *40*, 1415-1422.
- [22] Dejun, L., Zhao, J. Surface modification of medical polyurethane by plasma treatment. *Chinese Phys. Lett.* **1992**, *9*, 79-82.
- [23] Occhiello, E., Morra, M., Morini, G., Garbassi, F., Humphrey, P. Oxygen-plasma-treated polypropylene interfaces with air, water, and epoxy resins. *J. of Appl. Polym. Sci.* **1991**, *42*, 551-559.
- [24] Wu, S. *Polymer Interface and Adhesion*, Marcel Dekker: New York, **1982**.
- [25] Zang, Z. Surface Modification by Plasma Polymerization and application of plasma polymers as biomaterials, Johanneses Gutenberg: University of Mainz, **2003**.
- [26] Abourayana, H., Zreiba, N., Elamin, A. Synthesis and characterization of plasma polymerized thin films deposited from benzene and hexamethyldisiloxane using (PECVD) method. *Eng. and tech.*, **2011**, *74*, 295-300.

DOCUMENT CONTROL DATA		
(Security markings for the title, abstract and indexing annotation must be entered when the document is Classified or Designated)		
1. ORIGINATOR (The name and address of the organization preparing the document. Organizations for whom the document was prepared, e.g., Centre sponsoring a contractor's report, or tasking agency, are entered in Section 8.)  <b>Defence Research and Development Canada – Atlantic</b> <b>9 Grove Street</b> <b>P.O. Box 1012</b> <b>Dartmouth, Nova Scotia B2Y 3Z7</b>		2a. SECURITY MARKING (Overall security marking of the document including special supplemental markings if applicable.)  <b>UNCLASSIFIED</b>
		2b. CONTROLLED GOODS  <b>(NON-CONTROLLED GOODS)</b> <b>DMC A</b> <b>REVIEW: GCEC DECEMBER 2012</b>
3. TITLE (The complete document title as indicated on the title page. Its classification should be indicated by the appropriate abbreviation (S, C or U) in parentheses after the title.)  <b>Tailoring wettability through the surface modification of electro-spun polymers by plasma and sol-gel treatments</b>		
4. AUTHORS (last name, followed by initials – ranks, titles, etc., not to be used)  <b>Gilmour, D.; Glendinning, R.; Kaye, B.; Saville, P.</b>		
5. DATE OF PUBLICATION (Month and year of publication of document.)  <b>November 2014</b>	6a. NO. OF PAGES (Total containing information, including Annexes, Appendices, etc.)  <b>38</b>	6b. NO. OF REFS (Total cited in document.)  <b>26</b>
7. DESCRIPTIVE NOTES (The category of the document, e.g., technical report, technical note or memorandum. If appropriate, enter the type of report, e.g., interim, progress, summary, annual or final. Give the inclusive dates when a specific reporting period is covered.)  <b>Scientific Report</b>		
8. SPONSORING ACTIVITY (The name of the department project office or laboratory sponsoring the research and development – include address.)  <b>Defence Research and Development Canada – Atlantic</b> <b>9 Grove Street</b> <b>P.O. Box 1012</b> <b>Dartmouth, Nova Scotia B2Y 3Z7</b>		
9a. PROJECT OR GRANT NO. (If appropriate, the applicable research and development project or grant number under which the document was written. Please specify whether project or grant.)  <b>12sz20</b>	9b. CONTRACT NO. (If appropriate, the applicable number under which the document was written.)	
10a. ORIGINATOR'S DOCUMENT NUMBER (The official document number by which the document is identified by the originating activity. This number must be unique to this document.)  <b>DRDC-RDDC-2014-R102</b>	10b. OTHER DOCUMENT NO(s). (Any other numbers which may be assigned this document either by the originator or by the sponsor.)	
11. DOCUMENT AVAILABILITY (Any limitations on further dissemination of the document, other than those imposed by security classification.)  <b>Unlimited</b>		
12. DOCUMENT ANNOUNCEMENT (Any limitation to the bibliographic announcement of this document. This will normally correspond to the Document Availability (11). However, where further distribution (beyond the audience specified in (11) is possible, a wider announcement audience may be selected.)  <b>Unlimited</b>		

13. **ABSTRACT** (A brief and factual summary of the document. It may also appear elsewhere in the body of the document itself. It is highly desirable that the abstract of classified documents be unclassified. Each paragraph of the abstract shall begin with an indication of the security classification of the information in the paragraph (unless the document itself is unclassified) represented as (S), (C), (R), or (U). It is not necessary to include here abstracts in both official languages unless the text is bilingual.)

The interaction of liquids with a material's surface is of fundamental importance to many processes including adhesion, chemical reactions, hydrodynamic transport, and surface cleanability. Surface properties can range from being hydrophilic, or oleophilic, where the liquid wets the surface and spreads, to superhydrophobic, or oleophobic, where the liquid beads on the surface and is easily displaced. The requirements for a surface to be superhydrophobic or oleophobic are low surface energies and minimal contact between the liquid and surface, which is often created by micron and nanometer scale roughness. In this work, solutions of polyurethane and polyvinylidene difluoride-co-hexafluoropropylene were electrospun to create mats of micron-sized fibres. Secondary roughness was added to the polymer fibres through the use of microphase separation, incorporation of nanoparticles, sol-gel reactions and by producing beads-on-a-string morphologies. Low surface energy was added by using fluorinated polymers, or through sol-gel reactions with low surface energy alkyl siloxanes, and plasma polymerization was attempted. Water contact angles of spun fibre mats were typically in the range of 110-130° which is hydrophobic, but the water drops were often pinned to the surface by fibres penetrating the drops. Sol-gel coatings resulted in water contact angles > 150° and very small tilt angles. Argon plasma treatment of the fibres resulted in water drops completely wetting the surface with very small contact angles. Better mass flow control of the monomer is required for plasma polymerization. Fibres were characterized by contact angle measurement with a digital microscope; scanning electron microscopy; FTIR and EDX spectroscopy.

L'interaction de liquides avec la surface des matériaux est d'une importance fondamentale pour de nombreux processus, dont l'adhésion, les réactions chimiques, le transport hydrodynamique et la nettoyabilité des surfaces. Les propriétés des surfaces peuvent se situer dans une gamme allant d'un caractère hydrophile ou oléophile, quand le liquide mouille la surface et s'étale, à un caractère superhydrophobe, ou oléophobe, quand le liquide perle à la surface et est facilement déplacé. Les conditions pour qu'une surface soit superhydrophobe ou oléophobe sont une faible tension superficielle et un contact minimal entre le liquide et la surface, qui est souvent créé par une rugosité à l'échelle micrométrique ou nanométrique. Pour le présent travail, nous avons électrofilé des solutions de polyuréthane et de poly(difluorure de vinylidène-co-hexafluoropropylène) afin de créer des mats de fibres micrométriques. Une rugosité secondaire a été ajoutée aux fibres de polymère grâce à l'utilisation d'une séparation de microphase, à l'incorporation de nanoparticules, à des réactions sol-gel et par la production de formes semblables à des perles enfilées. On a introduit une faible tension superficielle en utilisant des polymères fluorés ou grâce à des réactions sol-gel avec des alkylsiloxanes de faible tension superficielle, et tenté une polymérisation sous plasma. Les angles de contact avec l'eau des mats de fibres filées étaient typiquement dans la gamme 110-130°, ce qui est hydrophobe, mais les gouttelettes d'eau étaient souvent liées à la surface par des fibres les traversant. Les revêtements sol-gel ont produit des angles de contact avec l'eau > 150° et de très petits angles de déversement. Le traitement des fibres au plasma d'argon a formé des gouttelettes d'eau mouillant complètement la surface avec de très petits angles de contact. Un meilleur contrôle du débit massique du monomère est requis pour la polymérisation sous plasma. Les fibres ont été caractérisées grâce à des mesures de l'angle de contact par microscopie numérique, par microscopie électronique à balayage, par spectroscopie IRTF et EDX.

14. **KEYWORDS, DESCRIPTORS or IDENTIFIERS** (Technically meaningful terms or short phrases that characterize a document and could be helpful in cataloguing the document. They should be selected so that no security classification is required. Identifiers, such as equipment model designation, trade name, military project code name, geographic location may also be included. If possible keywords should be selected from a published thesaurus, e.g., Thesaurus of Engineering and Scientific Terms (TEST) and that thesaurus identified. If it is not possible to select indexing terms which are Unclassified, the classification of each should be indicated as with the title.)

Superhydrophobic; Sol Gel; Super Oleophobic